

Rensselaer Polytechnic Institute
Interlibrary Loan



ILLiad TN: 155029

Borrower: UUS

Lending String: MUU,KKS,*YRM,NDD,CAI

Patron: Quast, Caitlin

Journal Title: Materials Research Society symposia
proceedings

Volume: 235 **Issue:**

Month/Year: 1992 **Pages:** 503

Article Author:

Article Title: ; Analysis of Experiments in Helium
Microbeam Mixing

Imprint: New York ; North Holland, c1981-

ILL Number: 82624177



Ariel: 129.123.124.220



Call #: TA418.6 .P48 1992

Location: fb (copy pgs)

ARIEL

Charge

Maxcost: \$25.00IFM

Shipping Address:

ILS-Merrill Library

3045 OLD MAIN HILL/Rm118

Utah State Univ.

LOGAN,UT 84322-3045

Email: ILSRQST@usu.edu

Odyssey: 129.123.124.234

Ariel: 129.123.124.220

ANALYSIS OF EXPERIMENTS IN HELIUM MICROBEAM MIXING

JOHN B. DAVIS*, R.E. BENENSON* AND DAVID PEAK**

* Physics Dept., SUNY at Albany, Albany, NY 12222

**Physics Dept., Union College, Schenectady, NY 12308

ABSTRACT

We have continued to investigate ion-beam mixing in bilayer targets irradiated by 2-MeV He⁺ microbeams at room temperature. Although we have previously reported a linear dependence of interface width on dose for Cu/Al targets¹, more extensive results have not supported this conclusion. Within statistical uncertainty, it appears that the interface width in Cu/Al (1) is proportional to the square root of dose, at constant dose rate, (2) is larger in Al than in Cu, for the same dose, (3) is proportional to the 1/4 power of dose rate, and (4) is absent at liquid nitrogen temperature. Calculations of the expected interface growth rate from a radiation-enhanced diffusion model have provided order-of-magnitude agreement with observed rates. Additionally, intermixing of Cu and Al outside the damaged area may indicate significant transverse diffusion of vacancies.

INTRODUCTION

Ion-beam mixing processes generally fall into two fundamental categories, ballistic and thermal. Besenbacher found that when ballistic mixing is dominant, the RBS spectrum will have both long- and short-range components, corresponding to recoil and cascade mixing, respectively.² Our experiments have produced qualitatively similar results. However, calculations of the expected interdiffusion rate, derived from transport theory³, yield predictions which are at least an order of magnitude lower than we have observed.

An alternative mechanism for the He⁺ ion-beam mixing of Cu/Al is radiation-enhanced diffusion. In this process, vacancies and interstitials are produced by the ion beam at a rate P which may be calculated from Kinchin-Pease theory,

$$P = (0.4 \epsilon / N E_d) d\phi/dt \quad (1)$$

where ϵ is the energy deposited per unit length due to nuclear collisions, E_d is the displacement energy for vacancy formation, N is the atomic density and $d\phi/dt$ is the dose rate. In steady-state, the vacancy production rate is equal to the vacancy-interstitial recombination rate. For simplicity, we assume that the atomic fraction of vacancies f_v equals the fraction of interstitials. Then

$$f_v = (P / 4\pi R_{iv} N D_v)^{1/2} \quad (2)$$

where R_{iv} is the maximum radius for spontaneous vacancy-inter-

stitial recombination and D_v is the diffusion coefficient for vacancies. D_v is given by

$$D_v = D_0 e^{-Q/kT} \quad (3)$$

where Q is the activation energy for vacancy migration and D_0 can be determined from the jump distance, the jump frequency and the migration entropy.

We further assume that interstitials are not highly mobile even at room temperature, because they become trapped at fixed sinks such as grain boundaries. Thus, interstitials do not contribute significantly to the diffusion process. The radiation-enhanced diffusion coefficient can then be written as the product of the vacancy diffusion coefficient and the atomic fraction of vacancies, f_v found from eq. (3),

$$D_{RED} = D_v f_v \quad (4)$$

A characteristic diffusion length σ is related to the product of time t and the radiation-enhanced diffusion coefficient,

$$2\sigma = 2(2D_{RED}t)^{1/2} \quad (5)$$

where 2σ is defined as the width W of the mixed layer.

Combining eqs. (1) - (5) and replacing time t with $\phi/(d\phi/dt)$ yields an expression for W

$$W = [((8/N)(0.4\epsilon D_v/E_d 4\pi R_{i,v})^{1/2})^{1/2}] \phi^{1/2}/(d\phi/dt)^{1/4} \quad (6)$$

EXPERIMENTAL METHOD

Bilayer targets were prepared by evaporation of a 2500-Å Cu film on a thick substrate of Al foil. Targets were irradiated at room temperature with He⁺ beams at 2.0 MeV, to doses of 0.5 - 5 x 10¹⁹ ions/cm². In order to minimize the effects of shape distortions, the focused ion beam was rastered over an area 1 μm larger than the beam diameter. RBS spectra were taken *in situ* using the same beam but without rastering ("spot" mode), from the center of the damaged area. Typical sampling times were 5 minutes for every hour of bombardment.

RBS maps were made by rastering the beam across the target at the end of the irradiation phase. The RBS yield was recorded in as many as four "windows" of the spectrum, at each location on a 256 x 256 grid. Typical map dimensions were 50 μm x 50 μm.

The cross-section of the beam was measured in each experiment by stepping it across across a 5-μm electron microscope grid wire and recording the RBS yield at each step. The yield as a function of position was then used to deduce the beam profile and width. Dose rates were determined at the beginning of each experiment by measuring the RBS yield from the copper film and using the solid angle of the detector and the film thickness to calculate the number of incident particles. Since the diameter of the beam was typically 5 μm or less, the dose rates were on the order of 10¹⁵ ions/cm²/sec. In spite of the high dose rates, calculations predict no detectable increase in the sample temperature from beam heating.

These experiments were also performed at liquid nitrogen

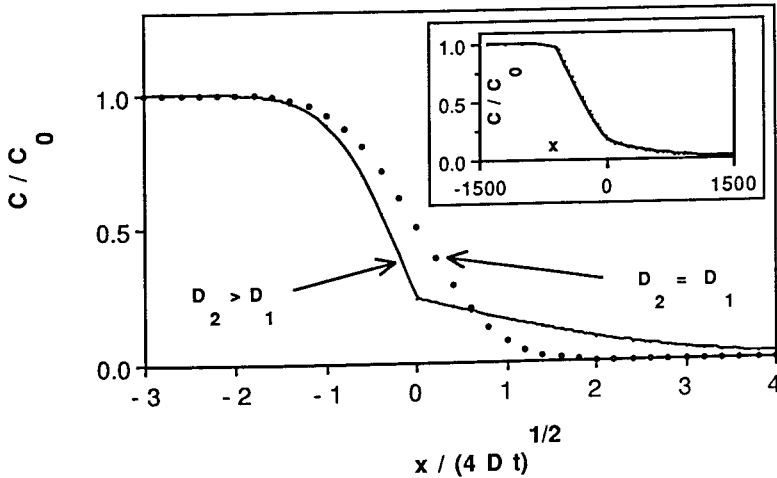


Fig. 1 - Concentration profile in a composite medium. Species are initially separated by a sharp interface at $x = 0$. D_1 and D_2 are diffusion coefficients for $x < 0$ and $x > 0$, respectively. Inset - Cu concentration as a function of distance (\AA) from interface, derived from RBS data for 2-MeV He^+ incident on Cu/Al target, after a dose of 5×10^{19} ions/ cm^2 .

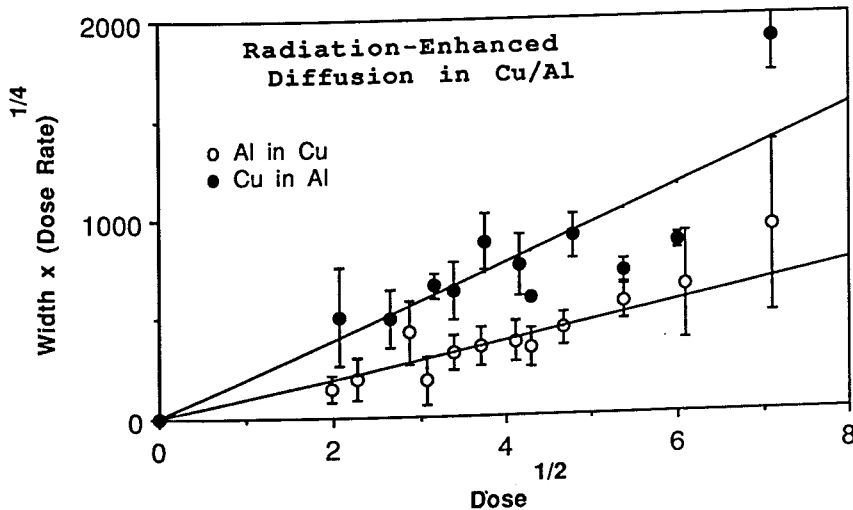


Fig 2. - The quantity $W(d\phi/dt)^{1/4}$ as a function of $\phi^{1/2}$. Widths (W) are measured in \AA , dose rates ($d\phi/dt$) in ions/ $\text{cm}^2/\text{min} \times 10^{18}$, and doses (ϕ) in ions/ $\text{cm}^2 \times 10^{18}$. The data are from several experiments for 2-MeV He^+ incident on Cu/Al, at different dose rates. Each point is the weighted average of a cluster of values with similar dose.

temperature, using a cryostat mounted directly to the movable stage at the end of the beam line.

RESULTS

Interface Discontinuity

We derived Cu concentration profiles from RBS spectra by successive iterations, using the analysis program RUMP. Typically, the profiles show a discontinuity at the location of the Cu/Al interface (Fig 1., inset), a feature which was overlooked in our earlier simulations, but which appears to be present in every profile. To first order, both the discontinuity and the obvious assymetry in the profile can be explained as the result of interdiffusion in a composite medium. The large graph in Fig. 1 compares the expected diffusion profiles for (1) two media with equal diffusion coefficients, and (2) the case where medium to the right of the interface has a larger diffusion coefficient than the medium on the left side. The form of the latter is qualitatively similar to the Cu concentration profile shown in the inset.

Interface Growth

The width W of the mixed layer on both sides of the interface was calculated from the Cu concentration profiles. On the Al side, the maximum concentration C_0 was assumed to be the Cu concentration at the interface. On the Cu side, C_0 was taken to be the initial Cu concentration before irradiation. On both sides, the width was defined as the distance between the 84% and 16% levels of C_0 .

Since the dose rates varied from one experiment to another, widths were multiplied by the 1/4 power of dose rate, in keeping with the form of eq. (6). Fig. 2 shows a graph of the quantity $W d\phi/dt^{1/4}$ as a function of $\phi^{1/2}$, for both the Cu and Al sides of the interface. The data were fitted to the equation

$$W (d\phi/dt)^{1/4} = \beta \phi^{1/2} \quad (7)$$

where the coefficient β is equivalent to the terms contained in square brackets in eq. 6. The experimental results for β are given in table I, together with the values used to calculate β from eq. 6.

Transverse Diffusion

Fig. 3 shows an RBS map of a damaged region of a Cu/Al target. It was recorded in a window of the spectrum just below the trailing edge of the Cu peak, where Cu atoms which have been displaced into the Al substrate are expected to appear. Although the He⁺ beam which produced the damage was 5 μm in diameter, the map clearly shows a structure at least two times larger. The size of the structure in comparison to the width of the mixed layer at the Cu/Al interface indicates that vacancies are migrating further from the damage cylinder in the transverse than in the longitudinal direction.

Further, the RBS yield is greatest outside the damaged

Table I - Summary of values used for eq. 6 and comparison of coefficient B from theory and experiment.

		<u>Cu</u>	<u>Al</u>
Atomic Density ($10^{22}/\text{cm}^3$)	N	8.45	6.02
Damage Energy* (10^6 eV/cm)	ϵ	3.0	4.5
Displacement Energy (eV)	E_d	30	45
Recombination Radius** (10^{-8}cm)	R_{iv}	11	12
Vacancy Migration Enthalpy ⁵ (eV)	Q	0.76	0.61
Diffusion Prefactor (cm^2/sec)	D_0	0.028	0.038
Coefficient B ($10^{-12}\text{cm}^{1/2}/\text{sec}^{1/4}$)			
experiment		11	22
theory (eq. 6)		1.1	4.6

*TRIM **Three times the lattice parameter

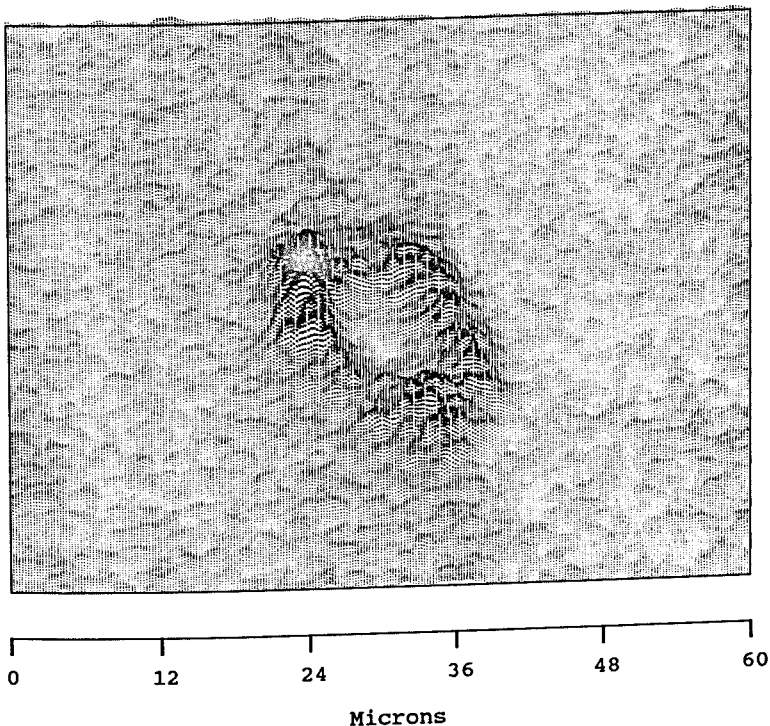


Fig. 3 - RBS map of a $60 \mu\text{m} \times 60 \mu\text{m}$ area of a Cu/Al target after irradiation with a $5\text{-}\mu\text{m}$, 2-MeV He^+ beam to a dose of 3.7×10^{19} ions/ cm^2 . The height of the map at any point is proportional to the RBS yield from a window of the spectrum below the low-energy edge of the Cu peak. The aiming point for the beam was approximately in the center of the map, and the beam center was rastered over a $1 \mu\text{m} \times 1 \mu\text{m}$ pattern during irradiation.

area, possibly indicating that the number of interstitials available for recombination is greater inside the damage cylinder than outside. Although interstitials are continually created by the ion beam, it is likely they are being trapped within a short distance of where they are produced. In that case, vacancies which diffuse beyond the damaged area will not often encounter an interstitial with which to recombine. Assuming the vacancies are not also trapped, they will diffuse into the material, away from the damage cylinder.

Low Temperature

When the same experiments were performed at liquid nitrogen temperature, no measurable changes were observed in the RBS spectra. We conclude from this that no ion-beam mixing of Cu and Al occurred at this temperature. This is perhaps the strongest piece of evidence in favor of the radiation-enhanced diffusion model. While ballistic mixing processes should by nature be independent of temperature, the vacancy diffusion coefficient at liquid nitrogen temperature is roughly 30 orders of magnitude smaller than at room temperature.

CONCLUSIONS

The disagreement between predicted and experimental values of the coefficient β is not surprising given the sensitivity of D_v to the exact value of Q . Nonetheless, it appears that at room temperature radiation-enhanced diffusion is the major contributor to He⁺ ion-beam mixing of bilayers. Although our studies have focused primarily on Cu/Al, preliminary results indicate the same process may operate in Cu/Si, Sb/Si and Mo/Si. At present, however, this model fails to take into account the concentration-dependence of the vacancy diffusion coefficients or the rate of interstitial trapping. As a result, questions remain about the rate of transverse diffusion.

REFERENCES

1. J. B. Davis and R. E. Benenson, in Surface Chemistry and Beam-Solid Interactions, eds. H. Atwater, F. Houle, D. Lowndes (Mat. Res. Soc. Proc. 201, Pittsburgh, PA, 1991) p. 245.
2. F. Besenbacher, J. Bottinger, S. K. Nielsen and H. J. Whitlow, App. Phys. A 29 141 (1982).
3. P. Sigmund and A. Gras-Marti, Nucl. Instr. and Meth. 182/183 25 (1981).
4. J. Crank, The Mathematics of Diffusion, 2nd ed. (Oxford Univ. Press, London, 1983), p. 38.
5. A. Seeger, D. Schumacher, W. Schilling and J. Diehl, eds. Vacancies and Interstitials in Metals (North-Holland, Amsterdam, 1970), pp. 255 - 361.